



# Hydrogen sulfide poisoning in solid oxide fuel cells under accelerated testing conditions

Ting Shuai Li, Wei Guo Wang, Tao Chen, He Miao, Cheng Xu\*

Division of Fuel Cell and Energy Technology, Ningbo Institute of Material Technology and Engineering, Chinese Academy of Sciences, 519 Zhuangshi Road, Ningbo, Zhejiang 315201, China

## ARTICLE INFO

### Article history:

Received 23 April 2010

Accepted 3 May 2010

Available online 12 May 2010

### Keywords:

Solid oxide fuel cell

Degradation

Hydrogen sulfide

Poisoning

Anode

## ABSTRACT

This study investigates the 0.2% hydrogen sulfide poisoning of Ni/YSZ anode-supported solid oxide fuel cells (SOFCs). The deterioration degrees and recovery extents of the cell current density, cell voltage and operation temperature are monitored. The results of impedance spectroscopy analysis show that hydrogen sulfide poisoning behavior may affect oxygen ion migration and gas diffusion and conversion on the anode side. Microstructural inspection reveals sulfur or sulfide formed on the anode-active area, which accounts for the immediate and severe cell power drop upon the injection of H<sub>2</sub>S. The nickel sulfide in the anodic functional layer cannot be completely removed after long-term regeneration and thus may be a key factor in the permanent degradation of the cell.

© 2010 Elsevier B.V. All rights reserved.

## 1. Introduction

A typical solid oxide fuel cell (SOFC) consists of a solid electrolyte, a cathode and an anode [1]. Extensive efforts have been invested in the research and development of SOFC anode materials, and the cermet Ni/YSZ is now widely studied as a commercial anode material candidate for SOFCs [2,3]. It has been shown that a cell fabricated using 50–60 wt% NiO balanced with YSZ as the active anode layer yields the best performance [2], which is highly associated with the particle size of the agglomerated NiO powder [3].

Although the Ni/YSZ cermet as an SOFC anode has exhibited great advantages due primarily to its high catalyst activity [4], there are still a number of challenges for its practical application in SOFCs, including its limited tolerance to sulfur [5–10] and other contaminants contained in coal syngas [11–13], oxidation–reduction intolerance [14,15] and vulnerability to carbon formation by exposure to hydrocarbon fuels [16]. Among these challenges, hydrogen sulfide (H<sub>2</sub>S) has been paid the most attention because of its immediate and severe detrimental effect on cell performance under various operating conditions [17,18]. Cheng et al. reported that the extent of H<sub>2</sub>S poisoning increased with a decrease in current density or an increase in cell voltage when the cell was fueled with hydrogen containing H<sub>2</sub>S concentrations ranging from 0 to 10 ppm at 800 °C [17], but they did not demonstrate whether this deteriora-

tion in cell performance was recoverable. Ishikura et al. investigated cell performance drop caused by exposure to H<sub>2</sub>S at concentrations of 0.1–20 ppm at 900 °C [18]. The results revealed that 20 ppm H<sub>2</sub>S in the fuel gas incurred permanent damage to the cell with a concurrent drop in output voltage to zero. This irrecoverable damage was attributed to reduction of the triple phase boundaries (TPBs) due to melted nickel sulfides. The promotion effect of liquid sulfur on nickel mobility was confirmed by Lussier et al. [19]; however, no nickel sulfide was found in the anode using XRD techniques.

To date, a number of investigations have been conducted on hydrogen sulfide poisoning behavior in SOFCs; nevertheless, very limited work has been carried out on the final tolerance of Ni/YSZ anodes to H<sub>2</sub>S at concentrations as high as 0.2% when the cell is operated at various current loads at 800 and 750 °C. This is imperative because the product syngas composition is fundamentally dependent on the coal and gasification processes, and the lowest concentration of H<sub>2</sub>S in raw syngas derived from the three major gasification systems is 0.2 vol.% [20]. On the other hand, the performance of SOFCs cannot be completely recovered (a condition known as permanent poisoning) by switching to sulfur-free gas after the cell is poisoned by concentrations of H<sub>2</sub>S higher than 20 ppm at 900 °C [18], and no methods have been proposed for remedying this partial performance recovery.

Research on the H<sub>2</sub>S poisoning mechanism not only is helpful in identifying sulfur poisoning conditions and contributing to the development of sulfur-tolerant materials as SOFC anodes [21–23], but it is also useful in understanding cell performance regeneration after switching to sulfur-free gas. Zha et al. investigated the partial regeneration of cell performance after exposure to 50 ppm

\* Corresponding author. Tel.: +86 574 86685139; fax: +86 574 87910728.  
E-mail address: [xucheng@nimte.ac.cn](mailto:xucheng@nimte.ac.cn) (C. Xu).

H<sub>2</sub>S in the fuel using electrolyte-supported button cells and found that the cell performance recovery after removing H<sub>2</sub>S from the fuel was fully or partially dependent on the operating conditions and duration of H<sub>2</sub>S exposure [24]. However, relatively few reports have been published concerning anode-supported cells exposed to H<sub>2</sub>S at much higher concentrations, especially cells with relatively large active areas, which possess great potential for commercial applications.

Accordingly, the present investigation was initiated to examine the poisoning effect caused by H<sub>2</sub>S at relatively large concentrations and the recovery features in typical Ni/YSZ anode-supported SOFCs. The effect of cell voltage, current density and operating temperature was systematically evaluated at an exposure of 0.2% H<sub>2</sub>S to determine the tolerance of Ni/YSZ-based anodes and to investigate H<sub>2</sub>S poisoning mechanisms under such accelerated testing conditions. The mechanism of permanent poisoning caused by H<sub>2</sub>S addition was studied by material analysis after the poisoning tests. Two different cooling routes were used after testing to explore the hydrogen sulfide poisoning mechanisms of the permanent and recoverable performance deteriorations.

## 2. Experimental

### 2.1. Cell fabrication

The anode-supported SOFC single cells used for the experiments were manufactured as a small series at the Division of Fuel Cell and Energy Technology at the Ningbo Institute of Material Technology & Engineering (NIMTE), Chinese Academy of Sciences. A 56% Ni-YSZ anode-supported layer and a 56% Ni-YSZ functional layer (~10 μm) were fabricated by tape casting to produce an anode substrate with a total thickness of nearly 400 μm. An 8YSZ (TOSOH Corp.) layer with a 10 μm thickness was printed on the anode as an electrolyte, and a double cathode consisting of a YSZ-LSM (LSM powder was prepared at NIMTE) composite active layer with a 25 μm thickness and an LSM current collecting layer that was about 30 μm thick were then deposited. The as-fabricated cell had an active area of 15 cm × 15 cm and was cut into four samples of 5 cm × 5.8 cm that had active areas of 4 cm × 4 cm for the tests. The procedures for cell preparation and LSM powder synthesis were described in detail in [25,26].

### 2.2. Single cell testing

The cells were tested using an alumina rig jointed with nickel and platinum foil as current collectors on the anode and cathode sides, respectively. For gas distribution, nickel foam was attached to the anode side, while an LSM-sandwiched silver net was on the cathode side. On each side of the cell, there was a contact Pt lead for potential measurements. Sealing was achieved using ceramic glass, and an additional 5.5 kg weight was applied to boost the sealing effect. The cells were heated to 850 °C in a furnace with a volume of 12 cm × 12 cm × 20 cm at a heating rate of 1 °C min<sup>-1</sup> in N<sub>2</sub> (0.1 SLM). The cells were then reduced at 850 °C with pure hydrogen (0.3–0.5 SLM) for 5 h to ensure that the NiO in the anode had been completely converted to Ni [27]. The cells were then cooled to 800 and 750 °C for electrochemical measurements. The testing facility is shown in Fig. 1.

### 2.3. Cell performance measurements

Current–voltage curves were characterized with 0.8 SLM H<sub>2</sub> as the anode fuel and 2 SLM air as the cathode gas. The cells were galvanostatically operated at 0.25, 0.4 and 0.6 A cm<sup>-2</sup> and potentiostatically at 0.6 and 0.75 V at 800 °C in a successive fashion. Each operating status was maintained for at least 10 h to avoid abrupt

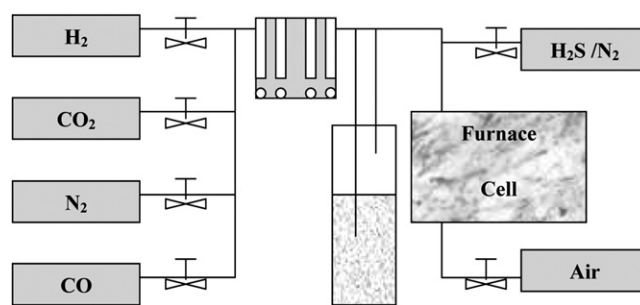


Fig. 1. Illustration of the testing facility.

electrode activation [28] before the cell was exposed to 0.2% H<sub>2</sub>S for 15 min. Comparative tests were conducted at 750 °C with the application of a constant current density of 0.25 and 0.4 A cm<sup>-2</sup>. The tests lasted for more than 1000 min until the terminal voltage reached an equilibrium state to observe the recovery features after switching to sulfur-free gas. Electrochemical impedance spectra (EIS) were acquired after H<sub>2</sub>S injection for 5 min at both 750 and 800 °C in potentiostatic mode using a sinusoidal signal with an amplitude of 20 mV over the frequency scanning range from 1 MHz to 0.1 Hz with an IM6ex electrochemical station. It was reported in previous investigations that the initial sulfur poisoning process mainly occurred within 5 min after H<sub>2</sub>S injection [29].

### 2.4. Microstructural analysis

After electrochemical tests, the cells were cooled to room temperature at the same rate for material analysis by two modes. In one mode, the cell was cooled in an H<sub>2</sub>/N<sub>2</sub> atmosphere after operating with sulfur-free gas for more than 1000 min, while in the other mode, the cell was immediately cooled in pure N<sub>2</sub> after injecting H<sub>2</sub>S for 15 min. All the microstructural analyses were carried out using a Hitachi S4800 field emission scanning electron microscope (FE-SEM/EDS).

## 3. Results and discussion

### 3.1. Effects of operating current density and voltage

Fig. 2 shows the cell voltage and power density as a function of current density for a typical SOFC single cell. The cell was first stabilized in pure H<sub>2</sub> gas until a steady open circuit potential was obtained (usually above 1.05 V at temperatures of 750–800 °C). Since the cells used for the test were manufactured in series with

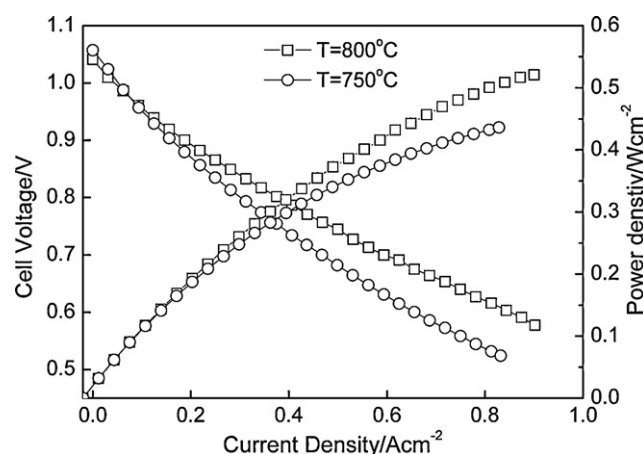
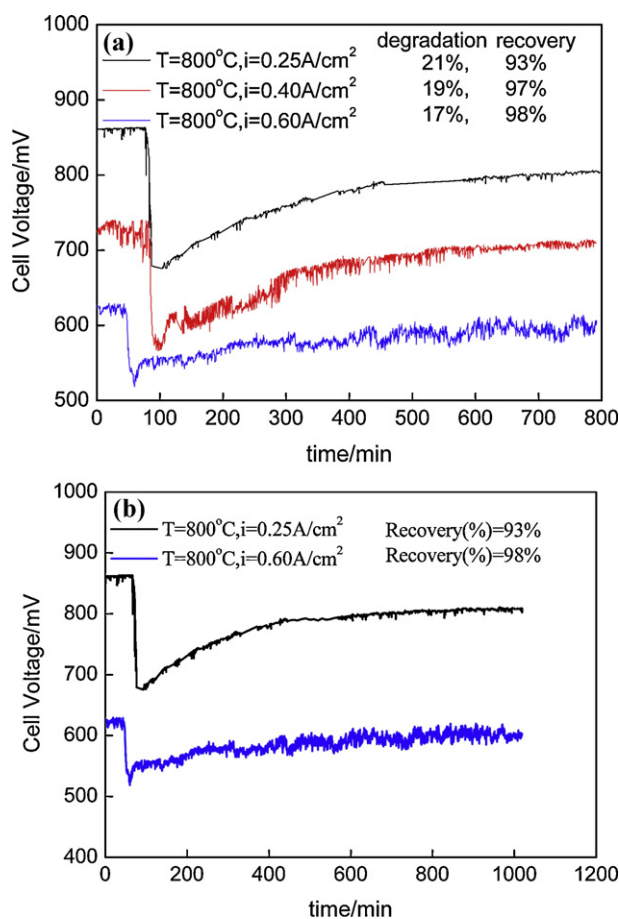


Fig. 2. Cell voltage and power density vs. current density recorded at 750 and 800 °C.



**Fig. 3.** (a) Effect of current density on  $\text{H}_2\text{S}$  poisoning and regeneration extent; (b) evaluation of extending the regeneration time for 200 min on the recovery degree.

relatively large active areas, the  $i$ - $V$  curves and power outputs shown in Fig. 2 represent average levels of the manufactured cells. The maximum power densities for the cells stabilized in hydrogen fuel were  $436\text{ mW cm}^{-2}$  at  $750^{\circ}\text{C}$  and  $520\text{ mW cm}^{-2}$  at  $800^{\circ}\text{C}$ . For comparison, the cell fabrication and operating conditions, including operation temperature, current density, cell terminal voltage and fuel flow, were kept identical. The performance drop was calculated using the ratio of the drop in cell current (or voltage for the galvanostatic mode) to the initial current value (or voltage for the galvanostatic mode).

The effect of current density on the  $\text{H}_2\text{S}$  poisoning behavior and performance regeneration extent at  $800^{\circ}\text{C}$  is demonstrated in Fig. 3(a). The deterioration rate increased from 17 to 21% with a decrease in current density from  $0.60$  to  $0.25\text{ A cm}^{-2}$  or an increase in voltage from  $0.63$  to  $0.86\text{ V}$ . However, the regeneration extent decreased from 98 to 93% of the initial cell voltage value after switching to sulfur-free gas for more than 10 h (about 700 min). The results indicated that a relatively high current density not only can reduce the  $\text{H}_2\text{S}$  poisoning effect, but also help with cell performance recovery. After removing the  $\text{H}_2\text{S}$  from the fuel, more water will be produced at the anode when the cell is operated at a higher current density load, which is helpful in recovering cell performance [8].

The observed deterioration trend caused by exposure to  $\text{H}_2\text{S}$  was similar to that reported by Cheng et al. [17]. However, they focused only on the degradation features caused by the addition of  $\text{H}_2\text{S}$  and paid no attention to the performance recovery characteristics. The present investigation was emphasized particularly on the recoverable extent after the cell was poisoned by a high concentration of  $\text{H}_2\text{S}$ , which can help in understanding the tolerance

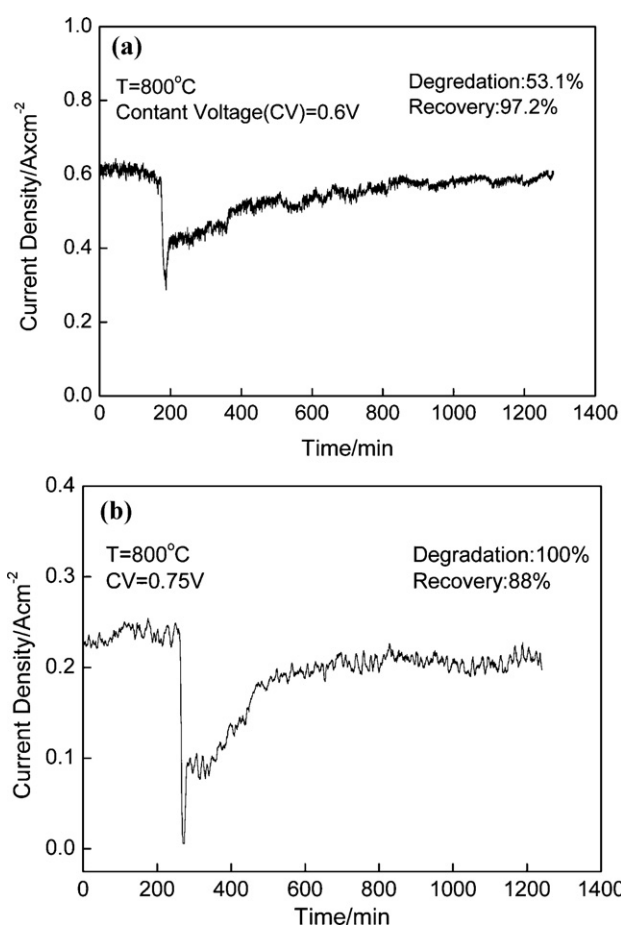


**Fig. 4.** Effect of cell voltage on  $\text{H}_2\text{S}$  poisoning and recoverable extent for the cell operated potentiostatically at (a)  $0.6\text{ V}$  and (b)  $0.75\text{ V}$ .

of Ni/YSZ anodes to  $\text{H}_2\text{S}$ . The results showed sharp declines in the cell voltages of 19 and 21% at constant current densities of  $0.25$  and  $0.4\text{ A cm}^{-2}$ , respectively, after exposure to  $0.2\%$   $\text{H}_2\text{S}$  for 15 min. This performance drop could be largely eliminated by switching to sulfur-free fuel, suggesting that this type of cell configuration can tolerate a low percentage of  $\text{H}_2\text{S}$  content in the fuel for short exposure time (15 min). An extra 200 min was added to observe the recovery process of cells operated at constant current densities of  $0.25$  and  $0.6\text{ A cm}^{-2}$ , as shown in Fig. 3(b). No further improvement was found in the recoverable extent. This indicated that a regeneration time of about 700 min was sufficient to reach equilibrium in this study.

The influence of cell voltage on sulfur poisoning and the regeneration process under the impact of  $0.2\%$   $\text{H}_2\text{S}$  is shown in Fig. 4. The extent of current density drop reached 53% upon the introduction of  $\text{H}_2\text{S}$  when the cell was operated potentiostatically at  $0.6\text{ V}$ . After removing sulfur gas for about 1000 min, the cell performance recovered to 97% to obtain a current density of  $0.62\text{ A cm}^{-2}$ . When the cell was operated potentiostatically at  $0.75\text{ V}$ , as shown in Fig. 4(b), the extent of sulfur poisoning was 100% and the recovery was about 88%, and the cell achieved a current density of  $0.25\text{ A cm}^{-2}$  after switching to sulfur-free gas for about 1000 min. It was apparent that the degradation increased with an increase in the cell voltage, but the extent of regeneration decreased with an increase of cell voltage from 88 to 97%. It appeared that the performance drop caused by the identical  $\text{H}_2\text{S}$  concentration was more severe under potentiostatic conditions than under galvanostatic conditions based on comparison of the results measured at a constant voltage of  $0.6\text{ V}$  and the results at a constant current density of  $0.6\text{ A cm}^{-2}$  ( $0.63\text{ V}$ ).

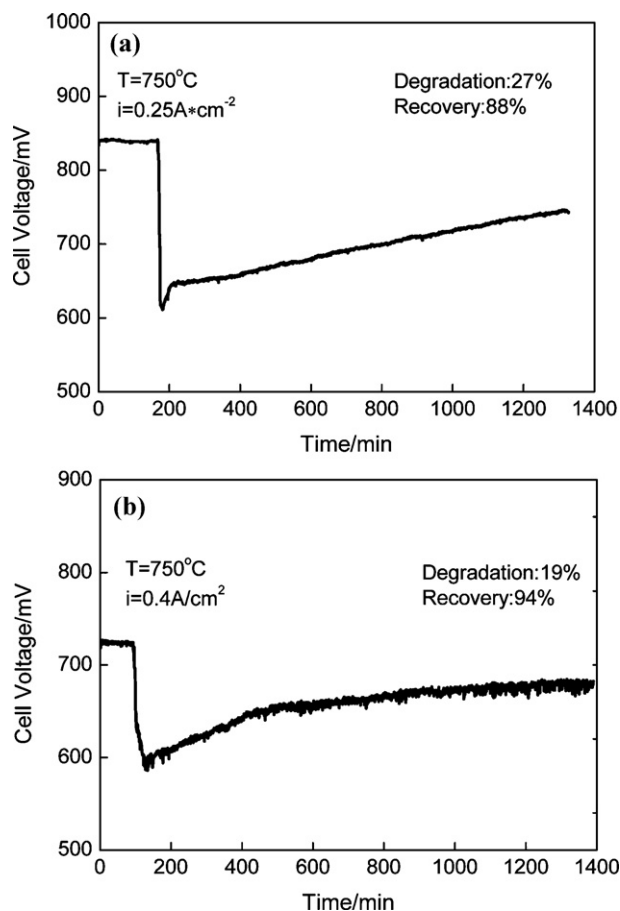


Fig. 5. Evaluation of  $\text{H}_2\text{S}$  poisoning behavior and recoverable extent at 750 °C for the cell operated galvanostatically at (a)  $0.25 \text{ A cm}^{-2}$  and (b)  $0.4 \text{ A cm}^{-2}$ .

However, the sharp drop in current density in the present investigation was not as severe as that reported by Zha et al., who observed a 16.67% decline in current density after exposure to 50 ppm  $\text{H}_2\text{S}$  within several minutes in  $\text{N}_2\text{-H}_2$  at 0.6 V, and a 12.7% decline in current density after exposure to 2 ppm  $\text{H}_2\text{S}$  within several minutes in  $\text{H}_2$  at 0.7 V [24]. This may be because the cell in [24] was an electrolyte-supported pellet cell, which makes  $\text{H}_2\text{S}$  much easier to transfer to the adjacent area of the electrolyte and directly attack the cell's active area.

The relationship of cell current density,  $i$ , and voltage,  $V_{\text{cell}}$ , can be expressed by the following equation:

$$V_{\text{cell}}(i) = \Delta E - iR - (\eta_a + \eta_c) \quad (1)$$

where  $V_{\text{cell}}(i)$  denotes the cell terminal voltage,  $\Delta E$  denotes the open circuit voltage or cell electromotive force,  $i$  denotes the cell current,  $R$  denotes the Ohmic resistance and  $\eta_a + \eta_c$  denotes the anode and cathode polarization (over potential) [1]. It is clear that the cell terminal voltage decreases with an increase in cell current density. Therefore, the relatively high current density corresponds to a relatively low cell voltage and has essentially the same influence on the  $\text{H}_2\text{S}$  poisoning behavior.

### 3.2. Effect of operation temperature

The effect of operation temperature on hydrogen sulfide poisoning and the recoverable extent was determined from the results in Figs. 3 and 5. The degradation was observed to be 27% when the cell was operated at 750 °C under a constant current density of  $0.25 \text{ A cm}^{-2}$ , as shown in Fig. 5(a), 6% higher than that at 800 °C under the same current density (Fig. 3(a)). At the same time, the

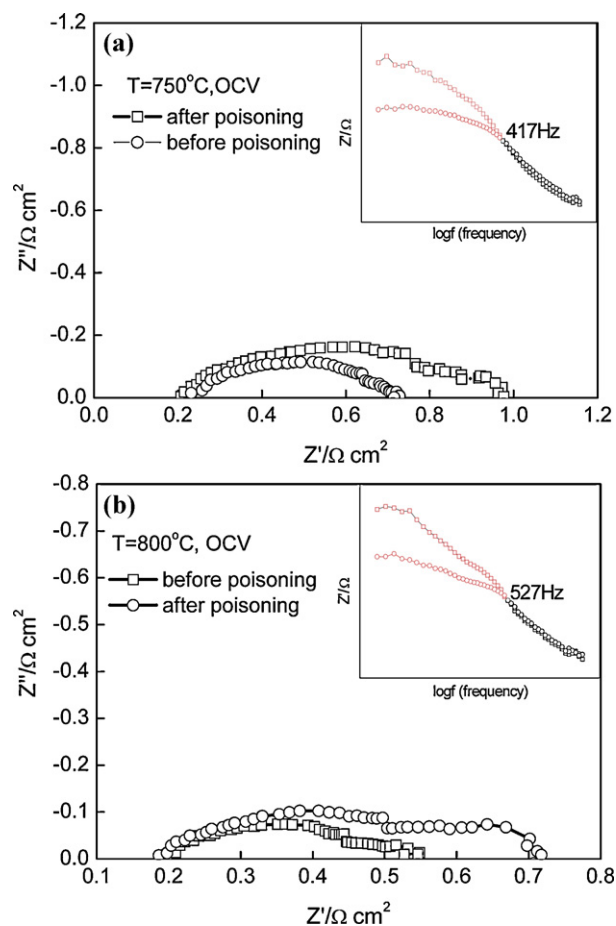
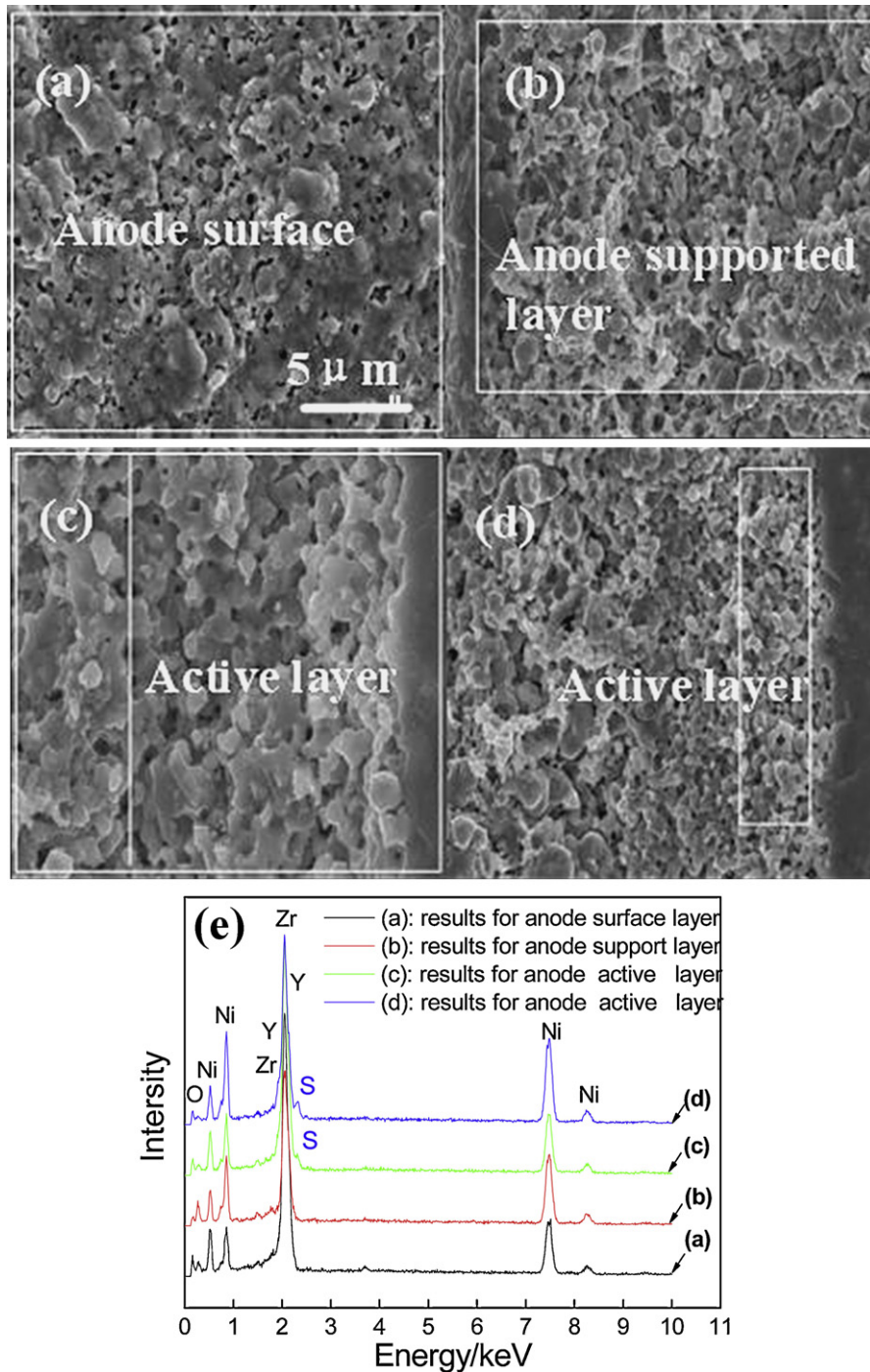


Fig. 6. Impedance spectra measured before and after  $\text{H}_2\text{S}$  poisoning at (a) 750 °C and (b) 800 °C.

performance recovery at 750 °C reached 88% of the initial cell voltage value, 5% lower than that at 800 °C. Upon increasing the current density to  $0.4 \text{ A cm}^{-2}$ , as shown in Fig. 5(b), the performance drop was 19%, and the regeneration extent reached 94%. It was clear that the degradation trend at 750 °C was almost the same as that at 800 °C, while the recoverable degree was elevated from 88 to 94% with a temperature increase from 750 to 800 °C. This trend for the degradation extent observed at  $0.4 \text{ A cm}^{-2}$  was somewhat contradictory to the results obtained at  $0.25 \text{ A cm}^{-2}$ , suggesting that operation temperature is not an independent factor influencing  $\text{H}_2\text{S}$  poisoning behavior.

The electrochemical impedance spectra (EIS) of the cells were measured in clean hydrogen fuel (before poisoning) and after the removal of  $\text{H}_2\text{S}$  (after poisoning), as depicted in Fig. 6, where  $Z_{\text{real}}$  is plotted against the logarithmic frequency to demonstrate the difference in the cell before and after poisoning. The evident increase in polarization resistance occurred at intermediate frequency and low frequency ranges, and the impedance spectra were different in frequency ranges below 417 Hz at 750 °C and below 527 Hz at 800 °C, respectively. These frequency ranges have been reported to be related to the desorption and adsorption of  $\text{O}_2$  and the transport to TPBs (summit frequency at 150 Hz for 700 °C and 1100 Hz for 850 °C), as well as diffusion and gas conversion at the anode (summit frequency below 10 Hz [30]). The series resistance showed no visible increase at the two temperatures, which implied that the operation temperature had no significant influence on the series resistance contributions, including the ionic and electronic conductivity of the cell or the contact between interfaces of the electrodes/electrolyte and electrodes/current collectors.



**Fig. 7.** Microstructures of the cell anode cooled to room temperature in  $H_2/N_2$  after long-term generation at (a) anode surface; (b) anode-supporting layer; (c) and (d) anode-active layer and (e) their elemental analysis results.

### 3.3. Microstructural characteristics

Microstructural analysis was carried out to explore the factors that resulted in the considerable and abrupt drop in cell performance once 0.2%  $H_2S$  was introduced and the irrecoverable degradation by long-term exposure to sulfur-free fuel gas. The cells after the tests were cooled to room temperature in two separate modes. First, single cells after poisoning with long-term regeneration were cooled in a  $H_2/N_2$  mixture (20%  $H_2/80\%$   $N_2$ ). The microstructure and elemental diagnosis of the cells are given in Fig. 7, where the upper region is an SEM image of the cell and the lower region is the EDS analysis results of the anode surface,

anode-supported layer and anode-active layer. No nickel sulfide was found on the anode surface or anode-supported layer, but sulfur was detected in the anode-active layer, and the sulfur content seemed to increase with a decreasing distance to the interface of the anode and electrolyte.

In order to observe the morphology of the sulfide, the anode-active zone was line scanned to locate the sulfide, as shown in Fig. 8(a). The sulfide was observed adjacent to the boundary between the anode-supporting layer and the anode-active layer. The S-rich area in Fig. 8(a) is marked by a white square and magnified in Fig. 8(b), where a cluster of particles with sizes of about  $0.01 \mu m$  are shown. The EDS analysis indicated that Ni and S were

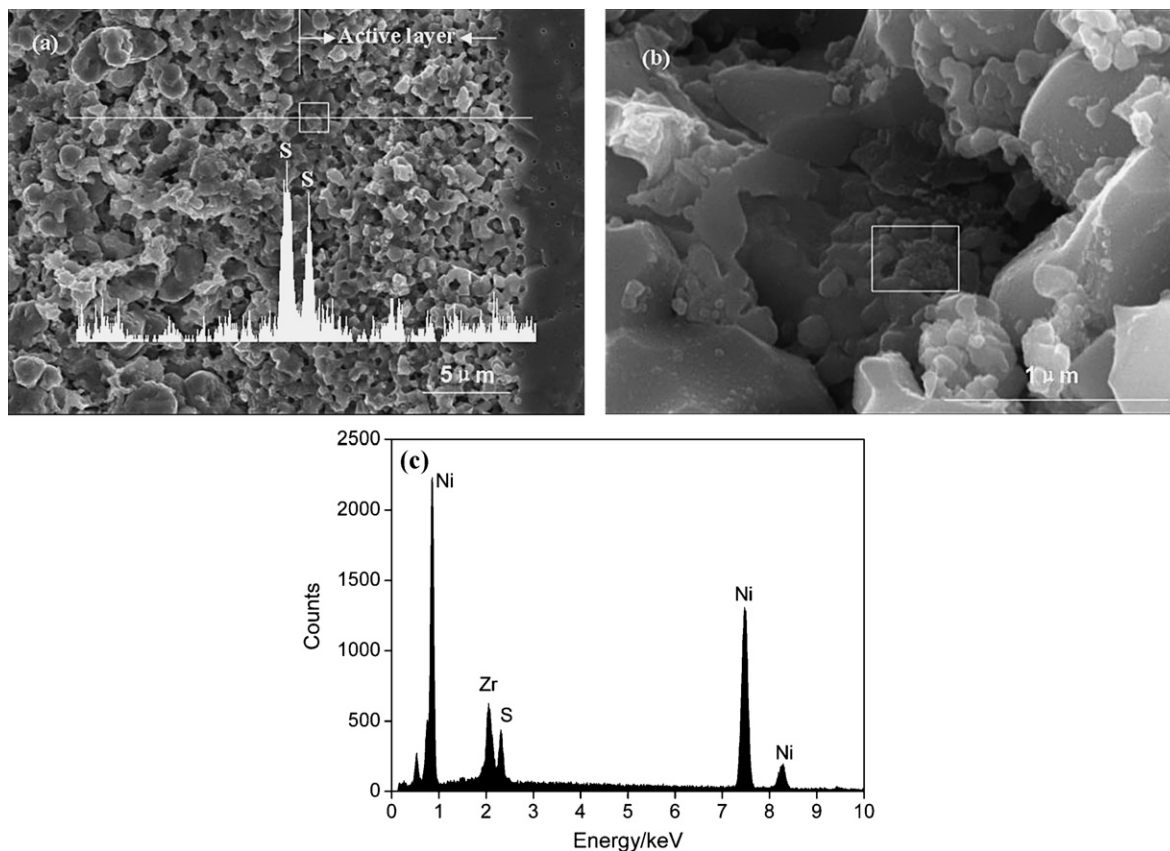


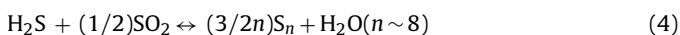
**Fig. 8.** Elemental analysis of the cell anode cooled to room temperature in  $H_2/N_2$  after long-term generation: (a) results of EDS using line scan mode, (b) observation of sulfur or sulfide morphology and (c) elemental analysis of area selected in (b).

the major compositions of these particles, suggesting that these particles might be nickel sulfide formed in the anode-active layer. It should be noted that the morphology of these nickel sulfide particles was different from the molten sulfide observed in [18,19]; therefore, the mechanism of  $H_2S$  poisoning proposed by Ishikura et al. [18] and Lussier et al. [19] cannot explain the poisoning behavior in the present investigation. Here, the irrecoverable degradation may originate from sulfur or sulfide remaining in the anode-active layer, which can be avoided or reduced by increasing the operation temperature or current density.

Second, the cell after poisoning without any regeneration was cooled to room temperature in pure  $N_2$  once the  $H_2S$  flow was switched off. The microstructure and EDS analysis results are shown in Fig. 9. No S was found on the anode surface or anode-supported layer, which is in accordance with the results from the cell cooled in the  $H_2/N_2$  mixture. A large amount of S was detected in the anode functional zone close to the interface of the anode and electrolyte. Closer inspection indicated that S was deposited on the nickel surface or reacted with nickel to form nickel sulfide, which was the key factor in the immediate cell voltage drop upon the introduction of  $H_2S$ .

#### 3.4. Hydrogen sulfide poisoning mechanisms

The chemical reactions involving  $H_2S$  under SOFC operation conditions are summarized as follows:



In Eqs. (2) and (3), the  $H_2S$  reacts with oxygen ions transferred through the electrolyte from the cathode side at the anode, while Eq. (4) occurs based on the products from Eq. (3) reacting with  $H_2S$ . The EIS analysis showed in Fig. 6 that the  $Z_{real}$  for the cell subjected to  $H_2S$  poisoning deviated from the  $Z_{real}$  for the unpoisoned cell at frequencies below 400–500 Hz, indicating that hydrogen poisoning is achieved by influencing the desorption and adsorption of  $O_2$ , transport to TPBs, and diffusion and gas conversion at the anode. This may confirm the occurrence of Eqs. (2) and (3), where the consumption of  $O^{2-}$  and the production of sulfur may have a negative effect on  $O^{2-}$  transfer. The EDS results revealed that S-rich regions lie close to the interface between the anode-supporting layer and active layer and the interface between the anode and electrolyte, indicating that reactions involving  $H_2S$  tend to take place in these regions. Thus,  $H_2S$  is oxidized to S at these sites, which directly reduces the TPB size and electrode reaction sites, thereby leading to an immediate performance drop.

$H_2S$  can also be thermally decomposed into elemental sulfur and hydrogen, as shown in Eq. (5):



However, no sulfur was found on the anode surface or anode-supporting layer, even though 0.2%  $H_2S$  was used in the test. It has been reported that nickel sulfide could not be detected by XRD when a cell was exposed to 100 ppm  $H_2S$  at 727 °C for 5 days [31]. Additionally, the sulfur amount may be reduced by reaction with air to form small quantities of NiO when the cells are cooled [19]. Nevertheless, the  $H_2S$  amount in [19] was much less than the  $H_2S$  concentration used in the present investigation. Therefore, the operation of Eq. (5) may not dominate the poisoning behavior because the decomposition at the anode surface and supporting

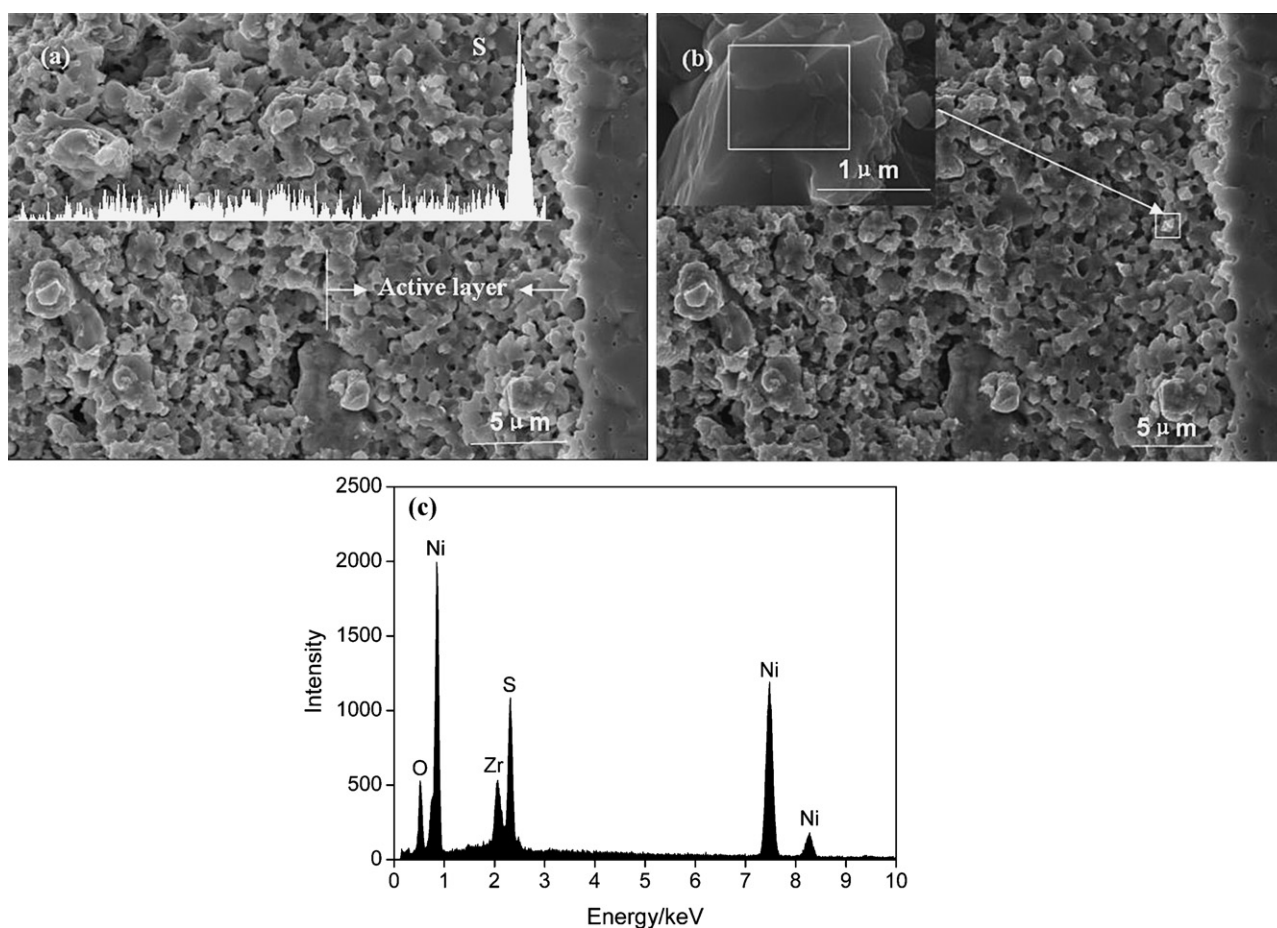


**Fig. 9.** Elemental analysis of the cell anode cooled to room temperature in  $N_2$  after switching off  $H_2S$  flow: (a) results of EDS using line scan mode, (b) sulfur or sulfide morphology and (c) elemental analysis of area selected in (b).

layer cannot be omitted with exposure to such a large concentration of  $H_2S$ .

The effect of current density, voltage and operation temperature on the  $H_2S$  poisoning behavior can be explained using the above reactions involving  $H_2S$ . The current density is related to fuel utilization by [32]:

$$I = -n^{el} \cdot U_f \cdot \dot{n}_{F1} \cdot F \quad (6)$$

where  $I$  denotes the cell current,  $n^{el}$  denotes the number of the electrons that are released during the ionization process of one utilized fuel molecule,  $U_f$  denotes the fuel utilization,  $\dot{n}_{F1}$  denotes the Mole-Flow at the anodic entrance and  $F$  is the Faraday constant. It can be seen that  $U_f$  is proportional to cell current (current density). Lussier et al. showed that the oxidation product at low  $U_f$  values tended to be sulfur, as shown by Eq. (2) [19], which results in a large performance drop. Conversely, the oxidation product at high levels of fuel utilization is sulfur dioxide, as presented by Eq. (3) [33]. The sulfur dioxide might be partially reduced to sulfur by  $H_2S$ , as shown by Eq. (4), accounting for a relatively small degradation degree. Upon the removal of  $H_2S$ , sulfur adsorbed on the nickel surface would be released based on thermodynamics [24]. Therefore, this process can be promoted by increasing the operation temperature. Also, Koch et al. reported that anode activation was generally more significant at higher current densities [34]. This anode activation may lead to performance regeneration in the cell poisoned by  $H_2S$ ; therefore, a higher current density would be beneficial to the regeneration process.

#### 4. Conclusions

The poisoning and regeneration behavior of typical anode-supported cells upon exposure to 0.2%  $H_2S$  have been investigated. The extent of  $H_2S$  poisoning increased with a decrease of cell current density and operation temperature, but increased with increasing cell voltage. The performance regeneration extent, however, increased with current density and operation temperature, but decreased with cell voltage. Sulfur detected in the anode-active zone may account for the immediate drop in cell voltage after injecting  $H_2S$ . The sulfur or sulfide in the anode-active layer cannot be completely removed at lower current densities and operation temperatures, resulting in irrecoverable degradation.

#### Acknowledgments

This work was accomplished at the Ningbo Institute of Material Technology & Engineering, Chinese Academy of Sciences, and was financially supported by the Qianjiang Program (No. 2008R10003), National 863 Program (No. 2007AA05Z140 and No. 2009AA05Z122) and the Ningbo Natural Science Foundation (Grant No. 50725101). Colleagues at the Division of Fuel Cell & Energy Technology are acknowledged for assistance in the single cell manufacturing process.

#### References

- [1] EG&G Technical Services, Inc. Under Contract No. DE-AM26-99FT40575, Fuel Cell Handbook, seventh edition, 2004.

- [2] J.R. Wilson, S.A. Barnett, *Electrochem. Solid-State Lett.* 11 (10) (2008) B181–B185.
- [3] C.X. Li, C.J. Li, L.J. Guo, *Int. J. Hydrogen Energy* 35 (2010) 2964–2969.
- [4] H. Koide, Y. Someya, T. Yoshida, T. Maruyama, *Solid State Ionics* 132 (2000) 253–260.
- [5] Z. Cheng, M. Liu, *Solid State Ionics* 178 (2007) 925–935.
- [6] K. Sasaki, S. Adachi, K. Haga, M. Uchikawa, J. Yamamoto, A. Iyoshi, J.T. Chou, Y. Shiratori, K. Itoh, *ECS Trans.* 7 (2007) 1675–1683.
- [7] J.N. Kuhn, N. Lakshminarayanan, U.S. Ozkan, *J. Mol. Catal. A: Chem.* 282 (2008) 9–21.
- [8] T.S. Li, H. Miao, T. Chen, W.G. Wang, C. Xu, *J. Electrochem. Soc.* 156 (12) (2009) B1383–B1388.
- [9] F.P. Nagel, T.J. Schildhauer, J. Sfeir, A. Schuler, S.M.A. Biollaz, *J. Power Sources* 189 (2009) 1127–1131.
- [10] J.F.B. Rasmussen, A. Hagen, *J. Power Sources* 191 (2009) 534–541.
- [11] J. Bao, G.N. Krishnan, P. Jayaweera, J. Perez-Mariano, A. Sanjurjo, *J. Power Sources* 193 (2009) 607–616.
- [12] K. Haga, S. Adachi, Y. Shiratori, K. Itoh, K. Sasaki, *Solid State Ionics* 179 (2008) 1427–1431.
- [13] H. Kuramochi, W. Wu, K. Kawamoto, *Fuel* 84 (2005) 377–387.
- [14] Y. Zhang, B. Liu, B. Tu, Y. Dong, M. Cheng, *Solid State Ionics* 176 (2005) 2193–2199.
- [15] A. Faes, A. Nakajo, A. Hessler-Wyserb, D. Duboisb, *J. Power Sources* 193 (2009) 55–64.
- [16] R.S. Gemmen, J. Trembly, *J. Power Sources* 161 (2006) 1084–1095.
- [17] Z. Cheng, S. Zha, M. Liu, *J. Power Sources* 172 (2007) 688–693.
- [18] A. Ishikura, S. Sakuno, N. Komiyama, H. Sasatsu, N. Masuyama, H. Itoh, K. Yasumoto, *ECS Trans.* 7 (2007) 845–850.
- [19] A. Lussier, S. Sofie, J. Dvorak, Y.U. Idzerda, *Int. J. Hydrogen Energy* 33 (2008) 3945–3951.
- [20] F.N. Cayana, M. Zhi, S.R. Pakalapati, I. Celik, N. Wu, R. Gemmen, *J. Power Sources* 185 (2008) 595–602.
- [21] X.C. Lu, J.H. Zhu, *J. Electrochem. Soc.* 155 (10) (2008) B1053–B1057.
- [22] H. Kurokawa, T.Z. Sholkapper, C.P. Jacobson, L.C. De Jonghe, S.J. Visco, *Electrochem. Solid-State Lett.* 10 (9) (2007) B135–B138.
- [23] S. Zha, P. Tsang, Z. Cheng, M. Liu, *J. Solid State Chem.* 178 (2005) 1844–1850.
- [24] S. Zha, Z. Cheng, M. Liu, *J. Electrochem. Soc.* 54 (2) (2007) B201–B206.
- [25] J.X. Wang, Y.K. Tao, J. Shao, W.G. Wang, *J. Power Sources* 186 (2009) 344–348.
- [26] Y. Tao, J. Shao, W.G. Wang, J. Wang, *FUEL CELLS* 09, no. 5, 2009, pp. 679–683.
- [27] T.S. Li, W.G. Wang, H. Miao, T. Chen, C. Xu, *J. Alloys Compd.* 495 (2010) 138–143.
- [28] V.A.C. Haanappel, A. Mai, J. Mertens, *Solid State Ionics* 177 (2006) 2033–2037.
- [29] K. Sasaki, K. Susuki, A. Iyoshi, M. Uchimura, N. Jingo, *J. Electrochem. Soc.* 153 (2006) A2023–A2029.
- [30] R. Barfod, A. Hagen, S. Ramousse, P.V. Hendriksen, M. Mogensen, *FUEL CELLS* 6, 2006, pp. 141–145.
- [31] J. Dong, Z. Cheng, S. Zha, M. Liu, *J. Power Sources* 156 (2006) 461–465.
- [32] S.C. Singhal, K. Kendall, *High Temperature Solid Oxide Fuel Cell-Fundamentals, Design and Applications*, 2003, Elsevier, P81.
- [33] D. Peterson, J. Winnick, *J. Electrochem. Soc.* 145 (1998) 1449.
- [34] S. Koch, M. Mogensen, P.V. Hendriksen, *Proceedings of the 6th European Solid Oxide Fuel Cell Forum*, 28 June–2 July 2004, Lucerne/Switzerland, 2004, p. 1000.